Extended thiophene chain for Ni-based porphyrin derivatives enabling high potential and long cycle life for electrochemical charge storage

Jiahao Zhang[a, #], Chao Ye[a, #], Yangmei Zhou[a], Caihong Sun[a], Tianfu Li[a], Xi Peng[a], Xiujuan Sun[a], Binhua Chen[b], Zhi Chen*[b], Ping Gao*[a]

[a.] *Key Laboratory of Environmentally Friendly Chemistry and Application of Ministry of Education School of Chemistry, College of Chemistry, Xiangtan University, Xiangtan 411105, China.*
**E-mail: ping.gao@xtu.edu.cn*
[b.] *College of Chemistry and Environmental Engineering, Shenzhen University, Shenzhen, Guangdong, 518060, China. E-mail: zhi.chen@szu.edu.cn*

Experimental Procedures

1.1 Materials：

All reagents and solvents were obtained from Alfa Aesar and Chemical Great-wall. Polyvinylidene fluoride (PVDF), acetylene black, stainless steel (316 L, 12 mm in diameter), *N*-methyl-2-pyrrolidone (NMP), and glass microfiber filters (Whatman, GF/D) were purchased commercially and used as received without further purification. The use of all glassware in the synthetic were conducted in oven-dried (70 °C).

1.2 Material characterization：

Mass spectrometry (MS) was performed on a Bruker Aupoflflex III Matrix-Assisted Laser Desorption Ionization Time of Flight Mass Spectrometer (MALDI-TOF MS) using α-cyano-4-hydroxycinnamic acid (CHCA) as the matrix. The morphology of samples was carried out using a field emission scanning electron microscope (SEM, JSM-6610LV). The attenuated total reflectance-Fourier transformation infrared (ATR-FTIR) spectroscopy was obtained on a Thermo Fisher Nicolet IS50 ATR-FTIR spectrometer from 600 cm^{-1} to 4000 cm^{-1}. UV-Vis spectra of porphyrins were measured on a Perkin–Elmer Cary 60 spectrometer. X-ray photoelectron Spectroscopy was recorded on an Escalab250Xi (Thermo Scientific), using monochromatized Al Kα radiation (1486 eV). The pass energy for survey spectra was 100 eV, for detail spectra the energy was 30 eV. The thermogravimetry–differential scanning (TGA) was

recorded on a Netzsch TG 209 (Netzsch). Cyclic voltammetry (CV) and electrochemical impedance using an electrochemical workstation (DH7000C, Jiangsu Donghua Analytical Instruments Co. Ltd.).

1.3 Electrochemical measurements:

The M-T_2TP electrodes were prepared by mixing 40 wt% acetylene black, 10 wt% PVDF, and 50 wt% of the active material (mass ratio). NMP was used as a solvent for preparing the slurry. Stainless steel was used as the current collector of porphyrin cathode. All electrodes were dried in a vacuum at 383 K for 12 hours before use. The M-T_2TP was used as cathode, alkali metal (Li, Na) foils were used as anodes and 1.0 M lithium hexafluorophosphate ($LiPF_6$) in propylene carbonate (PC) and 1.0 M $NaPF_6$ in PC were used as electrolytes. Whatman glass fiber was used as the separator. The mass load of the active substance is about 1.5 mg cm^{-2}. All capacities are calculated based on the active material of the electrode. The electrochemical redox potential was obtained by CV using an electrochemical workstation (CHI660E, Chenhua). The CR-2032 coin cell is assembled in an argon-filled glove box with oxygen and water concentrations below 0.01 ppm. The constant current charge and discharge test was conducted at the Neware battery test system (Neware, Shenzhen, China).

1.4 Synthesis of [5,10,15,20-tetra(2,2′-bithiophen-5-yl)porphyrinato] (H_2T_2TP):

A mixture of 40 mL propionic acid, 40 mL nitrobenzene, and 60 mL acetic acid was stirred at 138 ℃ and refluxed for 10 minutes. A mixed liquid (40 mL propionic acid and 10 g 2,2-biothiophene-5-acetaldehyde) was slowly injected. Then, a mixture of 40 mL acetic acid and 4.0 mL pyrrole was slowly added. After stirring for 90 min, the reaction mixture was poured into 100 mL MeOH and stirred at room temperature for 12 h in air. Afterward, the solid was filtrated by column chromatography (silica gel) using DCM:MeOH (49:1) as eluent. After recrystallizing from MeOH/DCM and drying

the product, a purple solid (7.2 g, 15%) was obtained. ^{1}H-NMR (500 MHz, $CDCl_3$, δ): –2.61 (s, 2H), 7.12 (dd, J = 3.6, 5.2 Hz, 4H), 7.34 (dd, J = 0.8, 5.2 Hz, 4H), 7.42 (dd, J = 0.8, 3.6 Hz, 4H), 7.58 (d, J = 3.6 Hz, 4H), 7.80 (d, J = 3.6 Hz, 4H), 9.17 (s, 8H); MALDI-TOF-MS Calc. for $C_{52}H_{30}N_4S_8$: $[M+H]^+$, 966.02; Found: m/z 966.84. UV-vis (CH_2Cl_2, nm) 441, 528, 569, 665.

1.5 Synthesis of [5,10,15,20-tetra(2,2′-bithiophen-5-yl)porphyrinato]nickel(II) (NiT_2TP):

$Ni(OAc)_2{\cdot}H_2O$ (0.487 g, 2.5 mmol) was added to a solution of compound H_2T_2TP (0.967 g, 1.0 mmol) in a mixture of 50 mL chloroform ($CHCl_2$) and 10 mL THF. Then it was heated at 60 ℃ for 36 h. After it was cooled to room temperature, it was poured into 150 mL water and extracted by DCM (150 mL). The DCM solution was concentrated under reduced pressure. The solid was filtrated by column chromatography (silica gel) using DCM:MeOH (49:1) as eluent. After the removal of solvents in vacuum, a purple solid NiT_2TP (0.971 g, 95%) was obtained. UV-vis (CH_2Cl_2, nm) 442, 543, 633. IR (KBr, cm^{-1}) 3097, 3070, 2927, 2855, 1598, 1553, 1526, 1421, 1346, 1223, 1074, 1044, 1010, 978, 790, 701. MALDI-TOF-MS Calc. for $C_{52}H_{28}NiN_4S_8$: $[M+H]^+$, 1021.94; Found: m/z 1021.78.

1.6 Synthesis of [5,10,15,20-tetra(2,2′-bithiophen-5-yl)porphyrinato]zinc(II) (ZnT_2TP):

$Zn(OAc)_2{\cdot}H_2O$ (0.504 g, 2.5 mmol) was added to a solution of compound H_2T_2TP (0.967 g, 1.0 mmol) in a mixture of 50 mL chloroform ($CHCl_3$) and 10 mL THF. Then it was heated at 60 ℃ for 36 h. After it was cooled to room temperature, it was poured into 150 mL water and extracted by DCM (150 mL). The DCM solution was concentrated under reduced pressure. The solid was filtrated by column chromatography (silica gel) using DCM:MeOH (49:1) as eluent. After the removal of

solvents in a vacuum, a purple solid ZnT_2TP (0.946 g, 92%) was obtained. UV-vis (CH_2Cl_2, nm) 444, 568, 633. IR (KBr, cm^{-1}) 3097, 3070, 2927, 2855, 1598, 1553, 1526, 1417, 1336, 1223, 1074, 1044, 1001, 978, 790, 692. MALDI-TOF-MS Calc. for $C_{52}H_{28}ZnN_4S_8$: $[M+H]^+$, 1027.94; Found: m/z 1027.86.

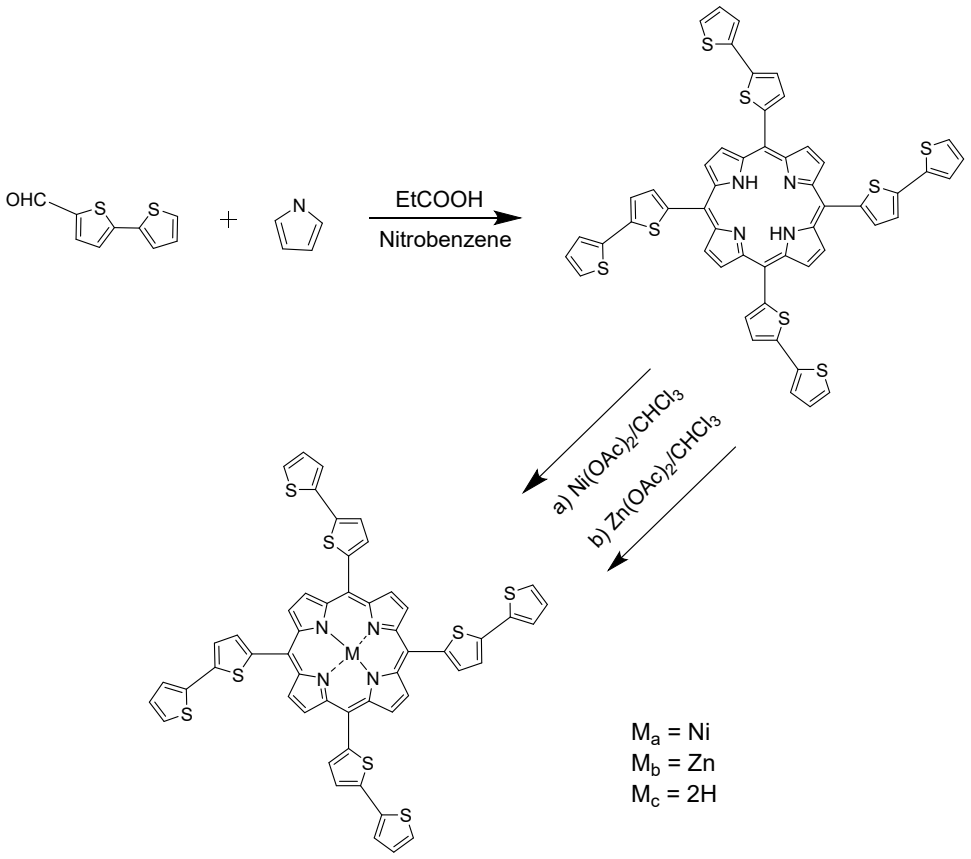

Scheme S1. Synthetic route and structure of MT_2TP (M_a = NiT_2TP, M_b = ZnT_2TP, M_c = H_2T_2TP).

Synthesis of [5,10,15,20-tetrathienylporphinato]nickel (II) (NiTTP):

1.7 Synthesis of 5,10,15,20-Tetrathienylporphyrin (H_2TTP):

A mixture of 10 mL propionic acid, 10 mL nitrobenzene, and 15 mL acetic acid was stirred at 138 ℃ and refluxed for 10 minutes. A mixed liquid (10 mL propionic acid and 1.35 mL thiophene-2-carbaldehyde) was slowly injected. Then, a mixture of 10 mL acetic acid and 1.35 mL pyrrole was slowly added. After stirring for 90 min, the reaction mixture was poured into 100 mL MeOH and stirred at room temperature for 12 h in air. Afterward, the solid was obtained by filtration and washed with a copious amount of ethanol and water. After the removal of solvents in a vacuum, a dark purple solid H_2TTP (1 g, 20%) was obtained. ^{1}H-NMR (500 MHz, $CDCl_3$, δ): –2.63 (s, 2H), 7.51 (dd, J = 3.2, 5.2 Hz, 4H), 7.86 (dd, J = 0.8, 5.2 Hz, 4H), 7.92 (dd, J = 0.8, 3.2 Hz, 4H), 9.04 (s, 8H); MALDI-TOF-MS Calc. for $C_{36}H_{22}N_4S_4$: $[M+H]^+$, 638.85; Found: m/z 639.29.

1.8 Synthesis of [5,10,15,20-Tetrathienylporphinato]nickel(II) (NiTTP):

$Ni(OAc)_2{\cdot}4H_2O$ (0.623 g, 2.5 mmol) was added to a solution of compound H_2TTP (0.319 g, 0.5 mmol) in a mixture of 50 mL chloroform ($CHCl_3$) and 10 mL THF. Then it was heated at 60 ℃ for 36 h. After it was cooled to room temperature, it was poured into 150 mL water and extracted by DCM (150 mL). The DCM solution was concentrated under reduced pressure. After the removal of solvents in a vacuum, a purple solid NiTTP (0.332 g, 95%) was obtained. UV-vis (CH_2Cl_2, nm) 423, 537. IR (KBr, cm^{-1}) 3099, 1552, 1430, 1330, 1301, 1235, 1168, 1075, 1035, 991, 860, 808, 793, 700. MALDI-TOF-MS Calc. for $C_{36}H_{20}NiN_4S_4$: $[M+H]^+$, 694.10; Found: m/z 694.07.

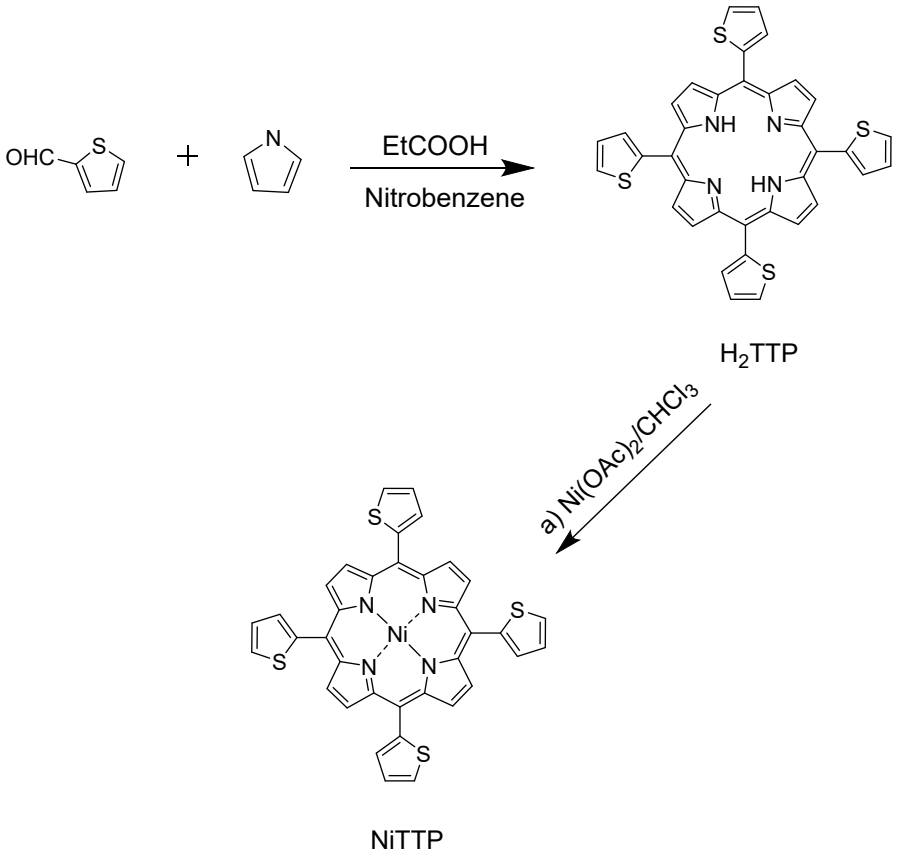

Scheme S2. Synthetic route and structure of NiTTP.

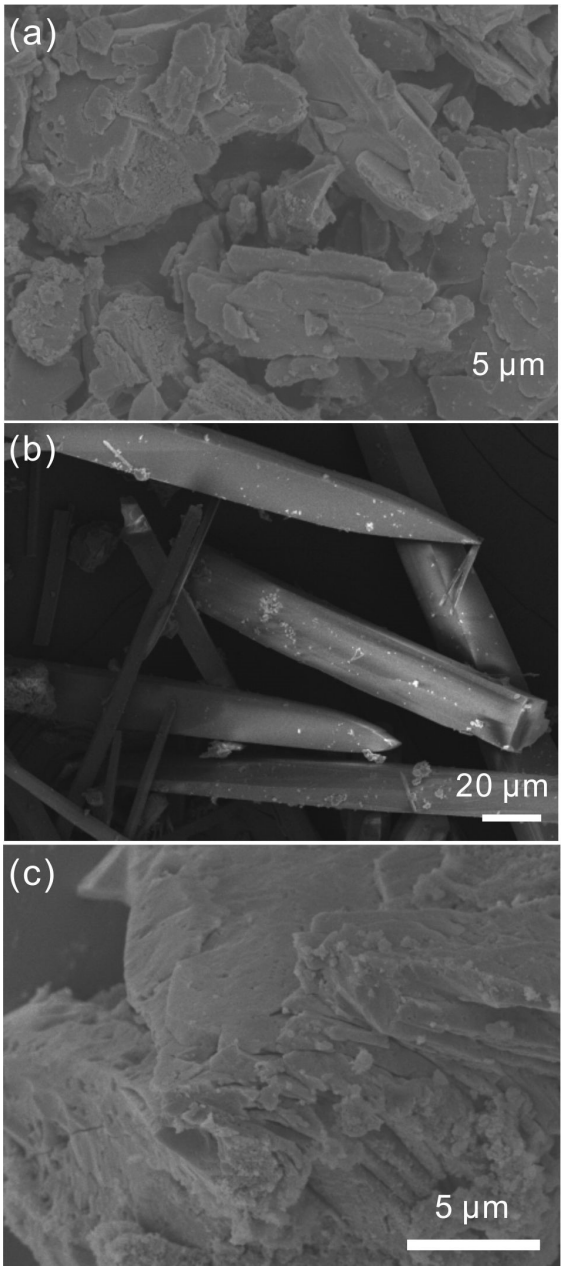

Figure. S1 SEM images of (a) H_2T_2TP, (b) NiT_2TP, (c) ZnT_2TP

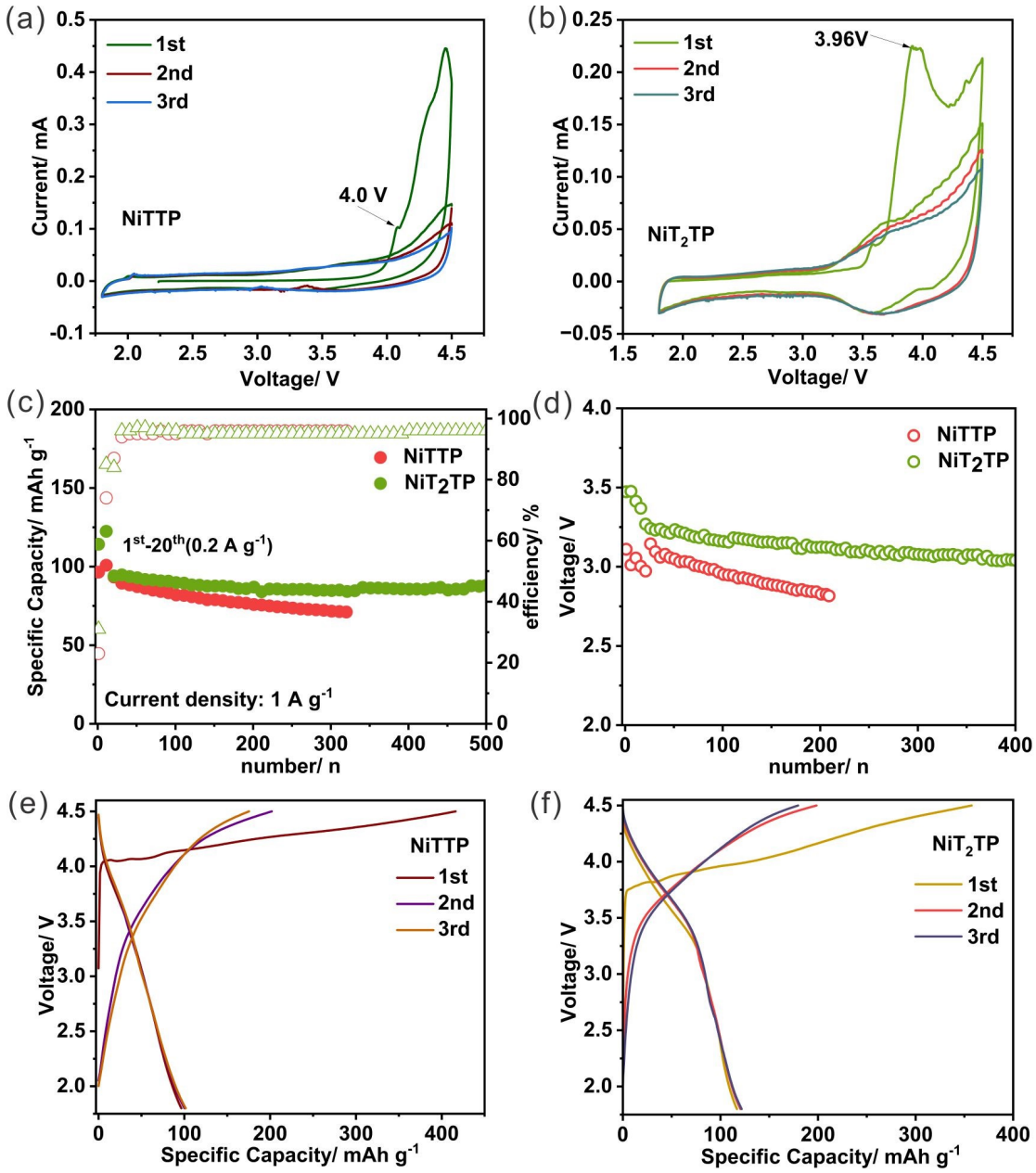

Figure. S2 (a,b) CV curves of NiTTP and NiT_2TP cathode at a scanning rate of 0.1 mV s^{-1}, the test was operated in a voltage range of 1.8-4.5 V (vs Na^+/Na). (c) Cycle performance of NiTTP and NiT_2TP cathode at 1000 mA g^{-1}. (d) Medium voltage of NiTTP and NiT_2TP at 1000 mA g^{-1}. (e,f) Initial charge-discharge curves of NiTTP and NiT_2TP cathode for organic sodium batteries at 100 mA g^{-1}.

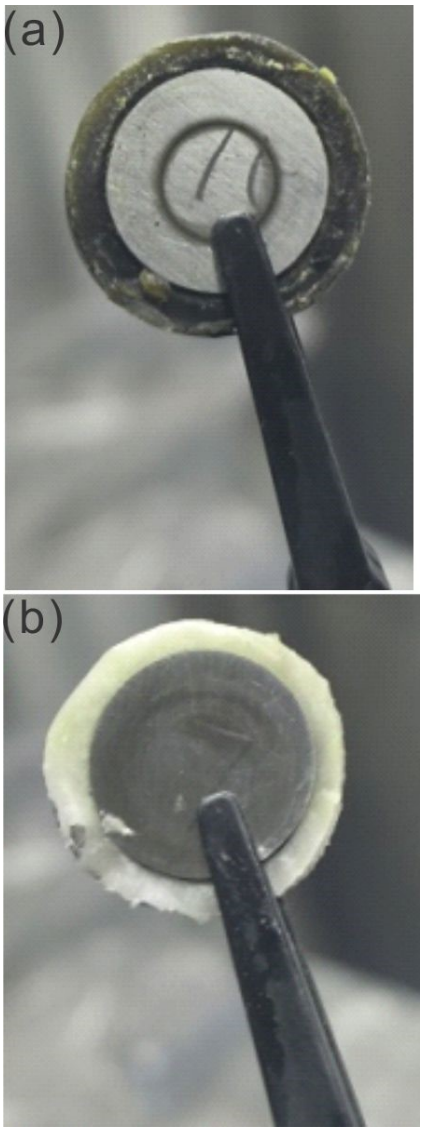

Figure. S3 The pictures of electrode materials in the first charged to 4.5 V (a) NiTTP, (b) NiT_2TP.

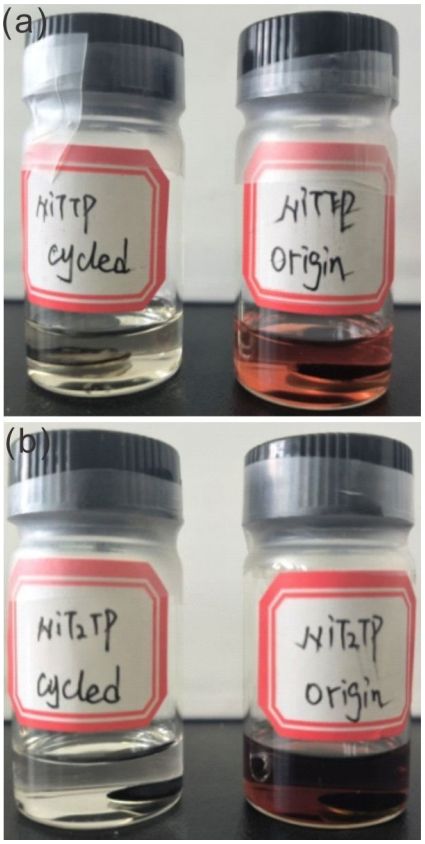

Figure. S4 The pictures of the as-prepared and cycled electrode material immersed in THF for 7 days. (a) NiTTP, (b) NiT_2TP.

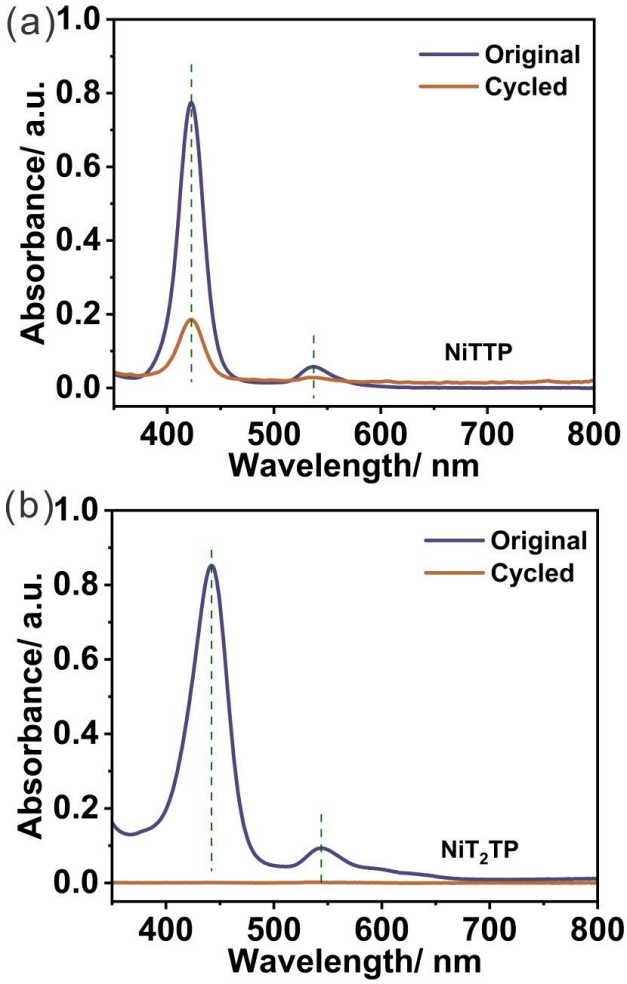

Figure. S5 The ex-situ UV-vis spectra of the as-prepared and cycled electrode material immersed in THF for 7 days. (a) NiTTP, (b) NiT_2TP.

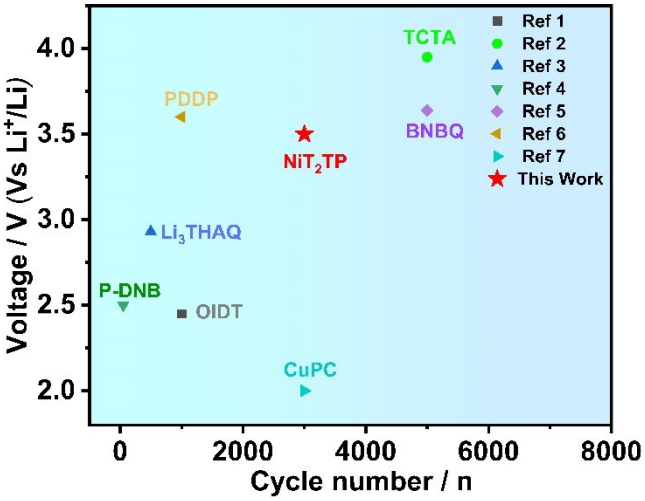

Figure. S6 The comparison voltage and cycle performance of NiT_2TP with the reported organic electrode materials.[1-8]

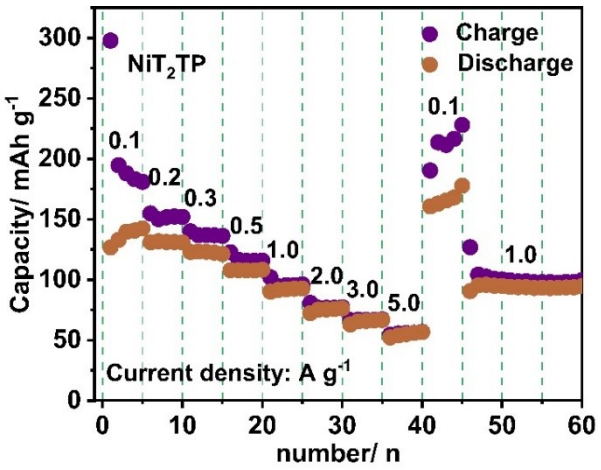

Figure. S7 Rate performance of NiT_2TP.

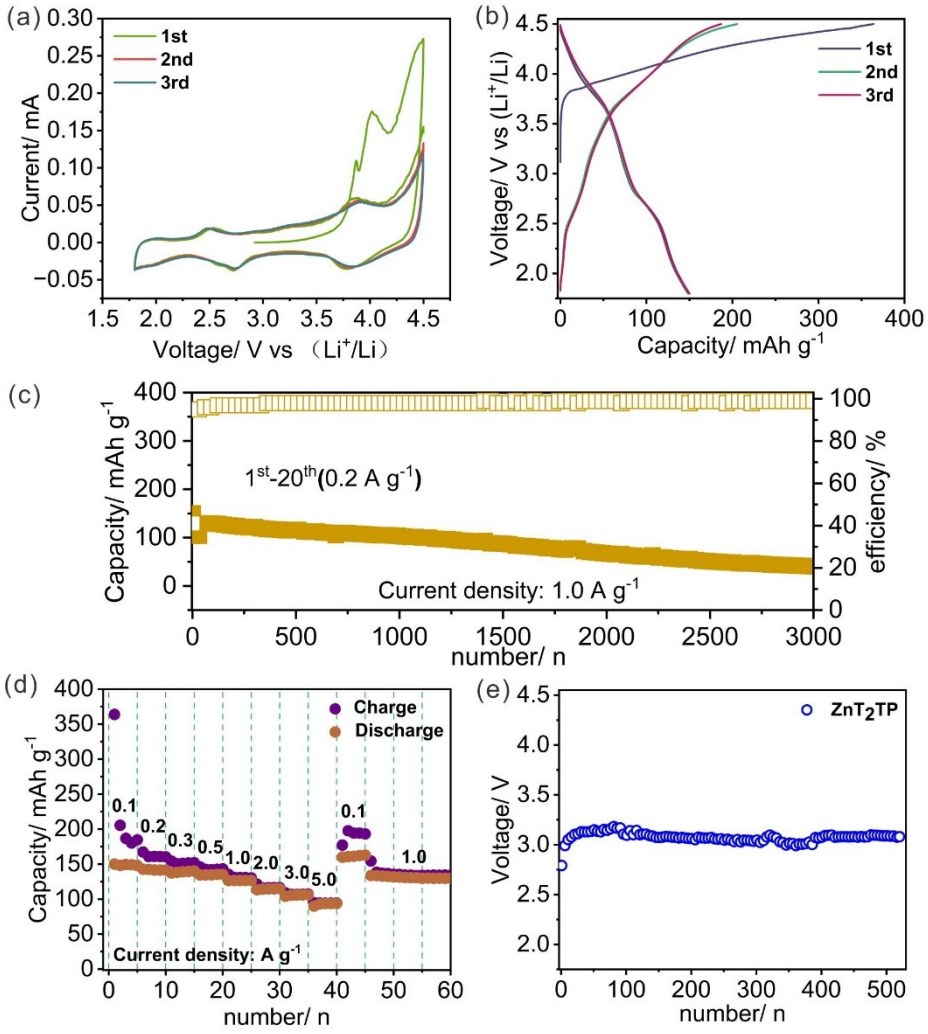

Figure. S8 (a) CV curves of ZnT_2TP cathode at a scan rate of 0.1 mV s^{-1}, the test was operated in a voltage range of 1.8-4.5 V (vs Li^+/Li). (b) Initial charge-discharge curves of ZnT_2TP cathode for organic lithium batteries at 100 mA g^{-1}. (c) Cycling performance of ZnT_2TP at 1000 mA g^{-1}. (d) The rate capability of ZnT_2TP electrodes. (e) Medium voltage of ZnT_2TP and H_2T_2TP at 1000 mA g^{-1}.

Comparing with NiT_2TP, the intensity of CV redox peaks of ZnT_2TP was relatively obvious, which indicated a multi-electron transfer process. The initial charge-discharge curves were consistent with the CV results and two inclined discharge platforms can be clearly observed, with an initial discharge capacity of 148 mAh g^{-1}. The rate performance also showed that ZnT_2TP had fast charge and discharge ability. However, ZnT_2TP undergoes a rapid capacity attenuation with a capacity retention of 31% when it was operated at a current density of 1.0 A g^{-1}, the fast capacity decay may be attributed to the structural instability of ZnT_2TP. As we can see, ZnT_2TP can also realize a high discharge voltage of 3.0 V.

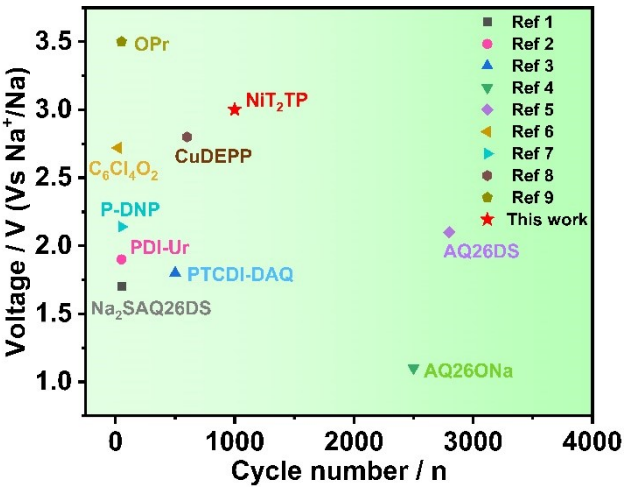

Figure. S9 The comparison voltage and cycle performance of NiT_2TP with the reported organic cathode electrode materials.[4,9-16]

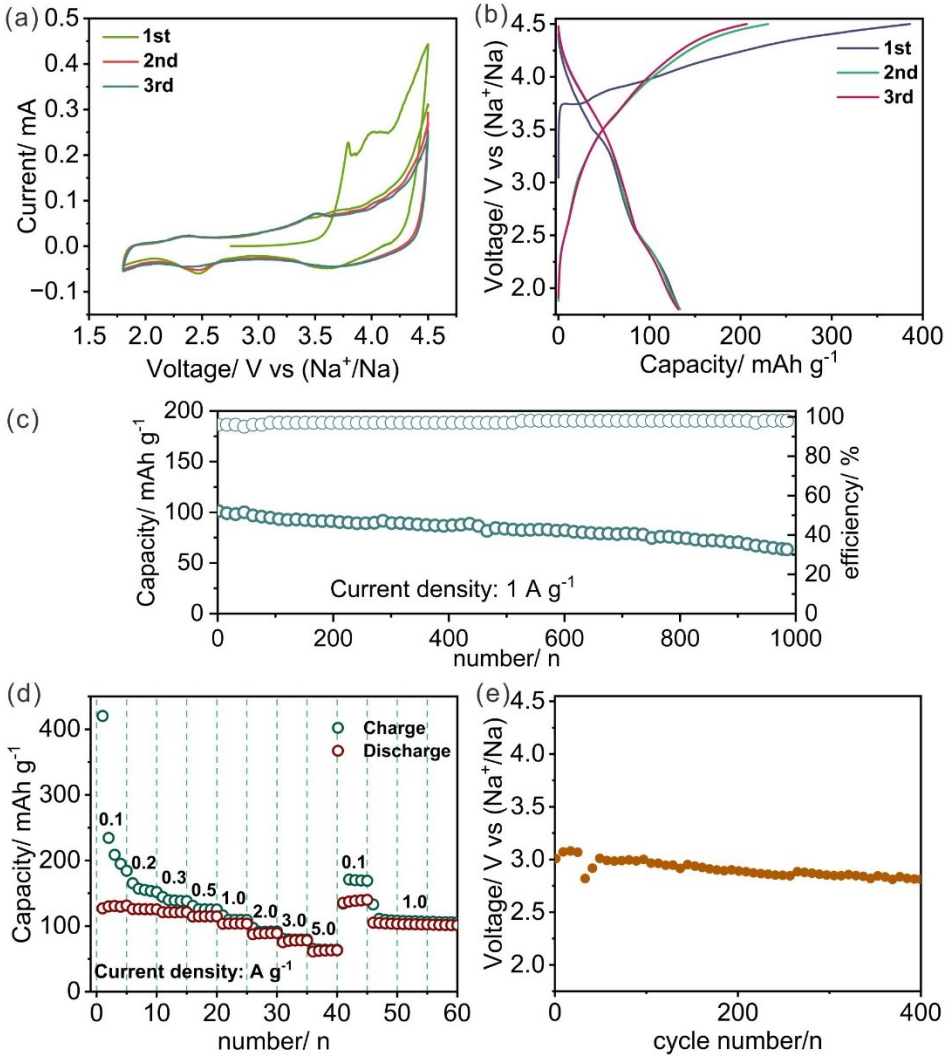

Figure. S10 (a) CV curves of ZnT_2TP cathode at a scan rate of 0.1 mV s^{-1}, the test was operated in a voltage range of 1.8-4.5 V (vs Na^+/Na). (b) Initial charge-discharge curves of ZnT_2TP cathode for organic sodium batteries at 100 mA g^{-1}. (c) Cycle performance of ZnT_2TP at 1000 mA g^{-1}. (d) Selected charge-discharge curves of ZnT_2TP at different cycles. (e) Medium voltage of ZnT_2TP at 1000 mA g^{-1} (vs Na^+/Na) .

The properties of ZnT_2TP in organic sodium batteries were also studied. The CV curves and initial three charge-discharge curves are alike with the results of ZnT_2TP in organic lithium-ion batteries, indicating a similar redox mechanism. The long cycle performance was operated at current density of 1.0 A g^{-1}, ZnT_2TP achieved a discharge capacity of 61 mAh g^{-1} up to 1000 cycles with a capacity retention of 61%. The rate performance also showed that ZnT_2TP had fast charge and discharge ability in organic sodium-ion batteries. As everyone knows, the median voltage of organic cathode materials in organic sodium batteries is often low, but ZnT_2TP can still achieve a high discharge voltage of 2.8 V after 500 cycles.

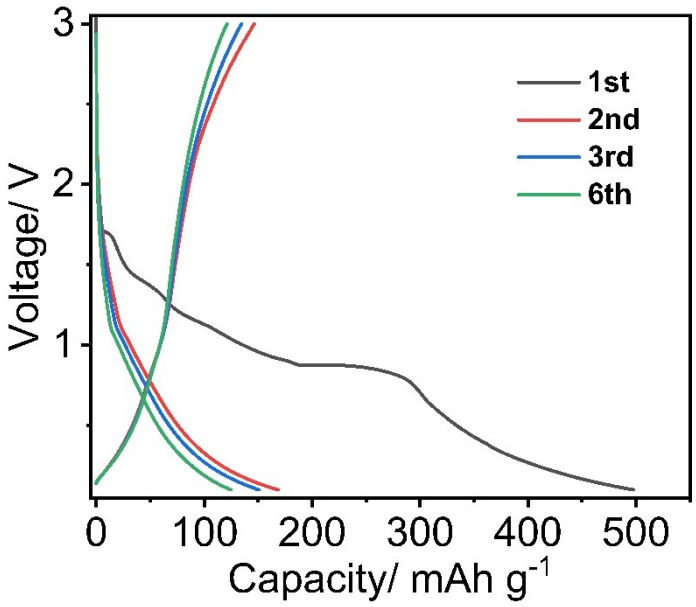

Figure. S11 Initial charge-discharge curves of NiT_2TP anode for organic lithium batteries at 100 mA g^{-1}.

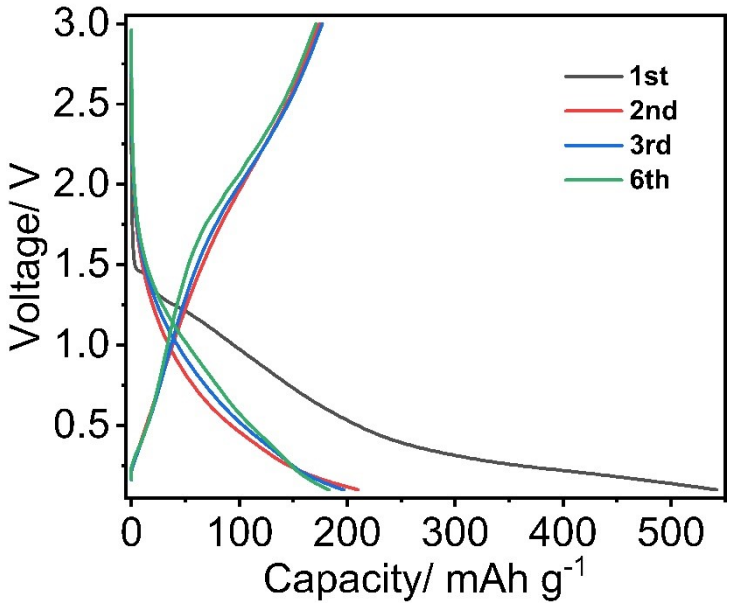

Figure. S12 Initial charge-discharge curves of NiT_2TP anode for organic sodium batteries at 100 mA g^{-1}.

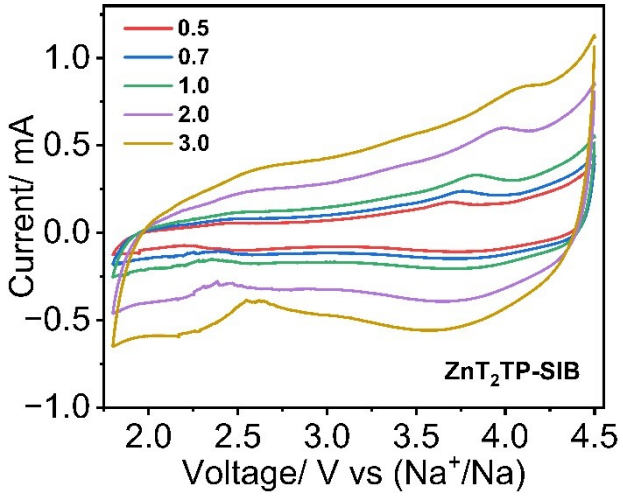

Figure. S13 The CV curves at various scan rates of ZnT_2TP in organic sodium batteries.

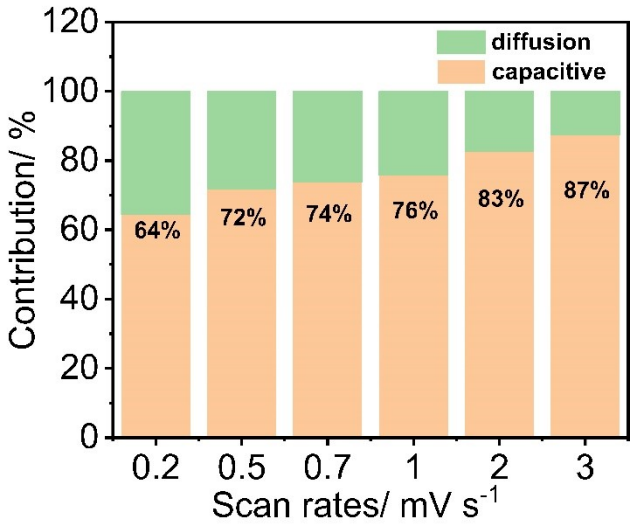

Figure. S14 The pseudocapacitance contribution of ZnT_2TP at different scanning rates.

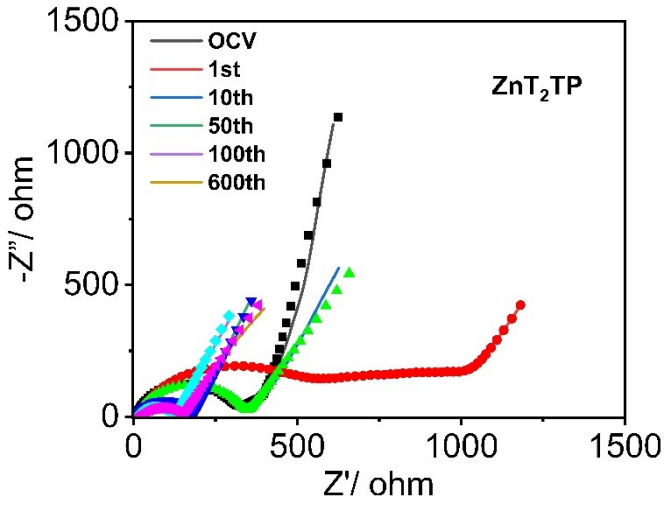

Figure. S15 The EIS spectra in the original, 1st, 10th, 50th, 100th, and 600th cycles of ZnT_2TP.

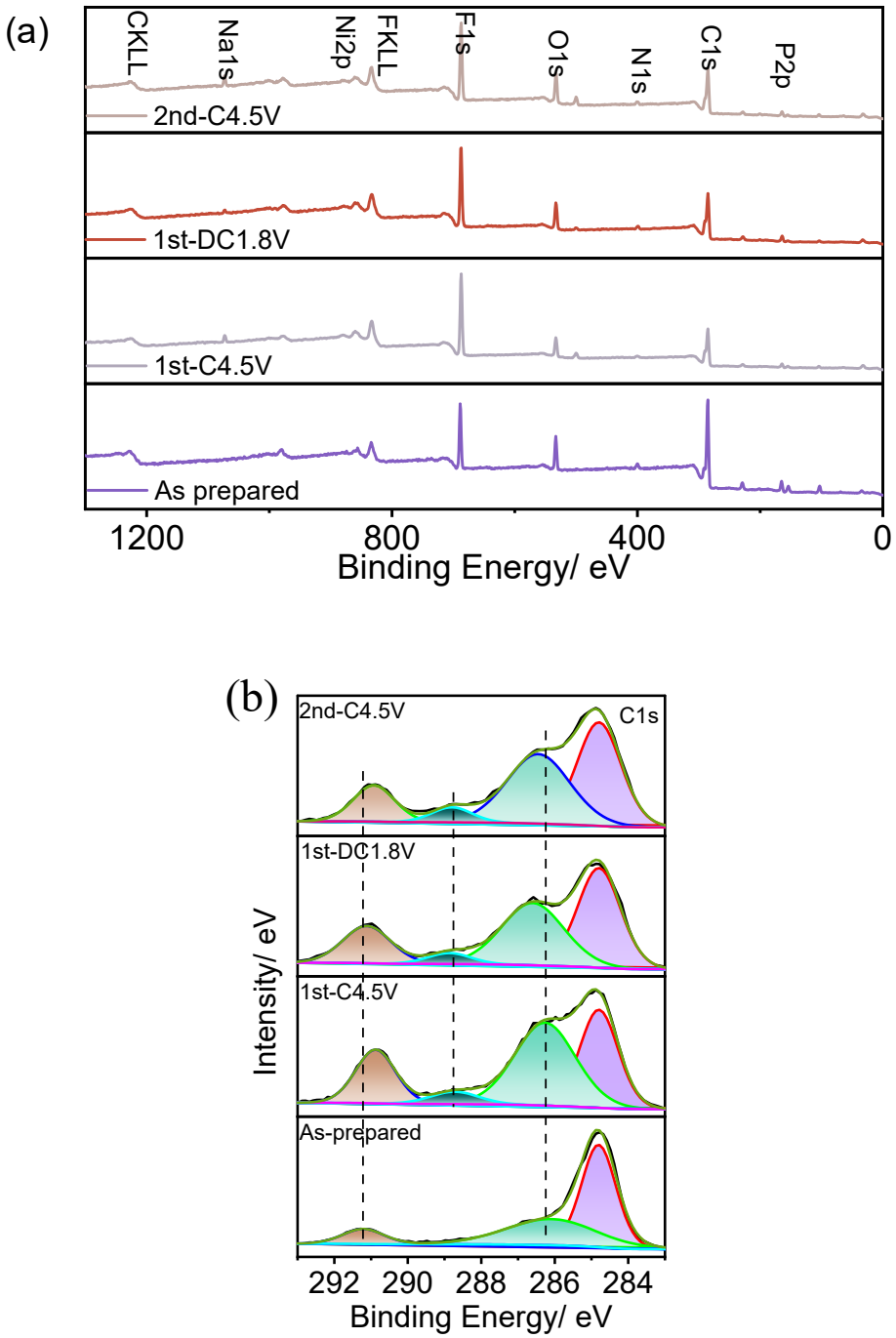

Figure. S16 (a) Survey XP spectra of NiT_2TP at as-prepared, charged, discharged, and re-charged states. (b) XP spectra core level of carbon in different cycled states.

References

1. T. Shi, G. Li, Y. Han, Y. Gao, F. Wang, Z. Hu, T. Cai, J. Chu and Z. Song, *Energy Storage Materials*, 2022, **50**, 265-273.
2. C. Zhao, Z. Chen, W. Wang, P. Xiong, B. Li, M. Li, J. Yang and Y. Xu, *Angewandte Chemie International Edition*, 2020, **59**, 11992-11998.
3. L. Huang, Z. Hu, M. Li, L. Luo, J. Wang, Y. Han, H. Zhan and Z. Song, *Chemical Engineering Journal*, 2024, **481** , 148447.
4. X. Liu and Z. Ye, *Advanced Energy Materials*, 2020, **11** ,2003281.
5. L. Zheng, J. Ren, H. Ma, M. Yang, X. Yan, R. Li, Q. Zhao, J. Zhang, H. Fu, X. Pu, M. Hu and J. Yang, *Journal of Materials Chemistry A*, 2023, **11**, 108-117.
6. C. Su, F. Yang, L. Ji, L. Xu and C. Zhang, *J. Mater. Chem. A*, 2014, **2**, 20083-20088.
7. H. Zhang, R. Zhang, X. Liu, F. Ding, C. Shi, Z. Zhou and N. Zhao, *Journal of Materials Chemistry A*, 2021, **9**, 24915-24921.
8. Y. Zhu, W. Jin, H. Gao, Y. Chen, T.-R. Wu, D.-Y. Wu, Y. Huang, D. Guo, Z. Chen, Q. Huang, J. Cao and J. Xu, *Chemical Engineering Journal*, 2023, **462** , 142229.
9. W. Tang, R. Liang, D. Li, Q. Yu, J. Hu, B. Cao and C. Fan, *ChemSusChem*, 2019, **12**, 2181-2185.
10. M. Ruby Raj, R. V. Mangalaraja, D. Contreras, K. Varaprasad, M. V. Reddy and S. Adams, *ACS Applied Energy Materials*, 2019, **3**, 240-252.
11. Y. Hu, Q. Yu, W. Tang, M. Cheng, X. Wang, S. Liu, J. Gao, M. Wang, M. Xiong, J. Hu, C. Liu, T. Zou and C. Fan, *Energy Storage Materials*, 2021, **41**, 738-747.
12. J. Hu, R. Liang, W. Tang, H. He and C. Fan, *International Journal of Hydrogen Energy*, 2020, **45**, 24573-24581.
13. W. Liu, W. Tang, X.-P. Zhang, Y. Hu, X. Wang, Y. Yan, L. Xu and C. Fan, *International Journal of Hydrogen Energy*, 2021, **46**, 36801-36810.
14. H. Kim, J. E. Kwon, B. Lee, J. Hong, M. Lee, S. Y. Park and K. Kang, *Chemistry of Materials*, 2015, **27**, 7258-7264.
15. X. Chen, X. Feng, B. Ren, L. Jiang, H. Shu, X. Yang, Z. Chen, X. Sun, E. Liu and P. Gao, *Nano-Micro Letters*, 2021, **13**, 71.
16. S. C. Han, E. G. Bae, H. Lim and M. Pyo, *Journal of Power Sources*, 2014, **254**, 73-79.